V.V. Abramov

A NEW SCALING FOR SINGLE-SPIN ASYMMETRY IN MESON AND BARION HADROPRODUCTION

Abstract

Abramov V.V. A New Scaling for Single-Spin Asymmetry in Meson and Baryon Hadroduction: IHEP Preprint 98-84. – Protvino, 1998. – p. 24, figs. 25, tables 9, refs.: 33.

Experimental data on single-spin asymmetries for inclusive meson and baryon production in proton-hadron collisions have been analyzed. It is found that the existing data can be described by a simple function of collision energy ($\sqrt{s}$), transverse momentum (p_T) and a new scaling variable $x_A = E/E^{BEAM}$. At beam energies above 40 GeV and p_T above 1.0 GeV/c single-spin asymmetries are described by a function of x_A and p_T only ($A_N = F(p_T)G(x_A)$) for both polarized proton fragmentation and central regions of proton-hadron collision. Discovery of this new scaling allows one to predict single-spin asymmetries for kinematic regions, not yet explored in experiments and to confront these predictions with future experiments and various models. The new scaling allows one also to use different reactions as polarimeters for experiments with polarized beam or target.

Аннотация

Абрамов В.В. Новая масштабная инвариантность для односпиновой асимметрии в образовании мезонов и барионов адронами: Препринт ИФВЭ 98-84. – Протвино, 1998. – 24 с., 25 рис., 9 табл., библиогр.: 33.

Проведен анализ экспериментальных данных по односпиновой асимметрии для инклюзивного образования мезонов и барионов в протон-адронных соударениях. Обнаружено, что существующие экспериментальные данные могут быть представлены в виде простой функции энергии соударения ($\sqrt{s}$), поперечного импульса (p_T) и новой скейлинговой переменной $x_A = E/E^{BEAM}$. При энергиях пучка выше 40 ГэВ и p_T выше 1,0 ГэВ/c односпиновые асимметрии описываются функцией только двух переменных x_A и p_T ($A_N = F(p_T)G(x_A)$), как для области фрагментации поляризованного протона, так и в центральной области протон-адронных соударений. Открытие этой новой масштабной инвариантности позволяет предсказать односпиновые асимметрии для кинематических областей, еще не исследованных в экспериментах и сопоставить эти предсказания с будущими экспериментами и различными моделями. Новая масштабная инвариантность позволяет использовать различные реакции как поляриметры для экспериментов с поляризованными пучком либо мишенью.

Introduction

Recent measurements have shown that at high enough energies single-spin left-right asymmetry for inclusive production of hadrons in reactions

$$h_1^{\uparrow} h_2 \to h_3 + X \tag{1}$$

where h_1, h_2 and h_3 are hadrons, is described by simple functions of kinematic variables and shows an approximate scaling in $x_F = 2p_Z^*/\sqrt{s}$ for fragmentation region of vertically polarized protons and scaling in $x_T = 2p_T/\sqrt{s}$ for central region [1]-[7]. Some authors have suggested that radial scaling exists for single-spin asymmetries ($x_R = 2p^*/\sqrt{s}$) [6,8], but a more careful study has not confirmed this, as will be shown below. The purpose of this study is to find a proper scaling variable, that allows one to describe in an unified way the dependence of single-spin asymmetries on kinematic variables in a wide range of beam energies, transverse momenta, and angles of particle production.

A thorough study of the existing data has shown that single-spin asymmetry for the inclusive π^+-meson production in $p^{\uparrow}p$ collisions has the following features [1,5,7]:

a) scaling and linear dependence on x_F or x_T in the region of polarized proton fragmentation or in the central region, respectively;

b) asymmetry maximum in the fragmentation region (near x_F=1) is approximately two times higher than it is in the central region (near x_T=1);

c) asymmetry changes its sign in the polarized proton fragmentation region at x_F near 0.18, while in the central region it happens at x_T near 0.37, which is approximately two times higher;

d) asymmetry grows with p_T rise at fixed x_F, has a plateau above 1 GeV/c, and probably decreases when p_T gets much higher 1 GeV/c;

e) asymmetry is zero at $p_T = 0$ due to the azimuthal symmetry of cross section.

Feature (d) has not too much experimental confirmation yet, but below it is assumed to be valid.

The features (b) and (c) are well explained if we assume that asymmetry is described by a new scaling variable:

$$x_A = E/E^{BEAM}, \qquad (2)$$

where E and E^{BEAM} are energies of the detected particle (π^+) and the beam particle (proton), respectively, in the laboratory reference system, where a polarized beam particle strikes a target at rest. This is because in the fragmentation region x_A is close to x_F and has maximum 1.0, while in the central region x_A is about $0.5 \cdot x_T$ and has maximum 0.5, when beam energy is divided between two high x_T jets (particles). In case of experiments with polarized target [7,9], x_A is calculated in antilaboratory reference system, where a beam particle is again a transversely polarized proton. Eq. (2) takes the form $x_A = p_{h_3} \cdot p_{h_2}/p_{h_1} \cdot p_{h_2}$ when it is expressed in the Lorentz-invariant way.

We expect that most of the above asymmetry features (a - e) are valid not only for π^+-production, but also for other pseudoscalar mesons (π^-, π^0, $K^\pm$, K_S, η), as well as for some baryons (protons, antiproton, hyperons), though experimental information for some of them is very limited. Thorough study of the available experimental data on single-spin asymmetries is presented in the next sections.

There are several variables which are numerically close to the x_A variable, given by eq. (2). In particular,

$$x_A' = (x_F + x_R)/2, \qquad (3)$$

$$x_A'' = (E + P_Z)/(E^{BEAM} + P_Z^{BEAM}), \qquad (4)$$

$$x_A''' = P/P^{BEAM}, \qquad (5)$$

where P and P^{BEAM} are momenta of the detected particle and beam particle, respectively, in the laboratory reference system. All of them are very close to each other at high energies and a choice of the best scaling variable requires additional and very accurate measurements of asymmetry. Eq. (3) gives a very transparent explanation of the x_F-scaling in the fragmentation region and the x_T-scaling in the central region.

1.   Asymmetry for $p^\uparrow p \to \pi^+ + X$ reaction

For the purpose of studying scaling features of single-spin asymmetry all the available experimental data are presented in the reference system in which a polarized proton is a projectile with spin directed upward and the target is at rest. Asymmetry is considered positive when most of particles are produced in the production plane to the left for the beam going downstream. So, the original sign of asymmetry for experiments [7,9] has been changed to opposite to match the above definition. Kinematic variables for the experiments which used polarized target have been transformed to antilaboratory reference system. Unfortunately, not all experiments presented in their publications a complete set of variables ($\sqrt{s}$, p_T, x_F) for each point. For some experiments only limits on these variables are given that makes transformation to other variables biased and limits accuracy of the x_A-scaling check. Additional error ($\epsilon = 0.025$) is added in quadrature to all points to take into account possible variable bias and systematic errors during fitting procedure below for π^+-meson and other particles if not stated otherwise.

2
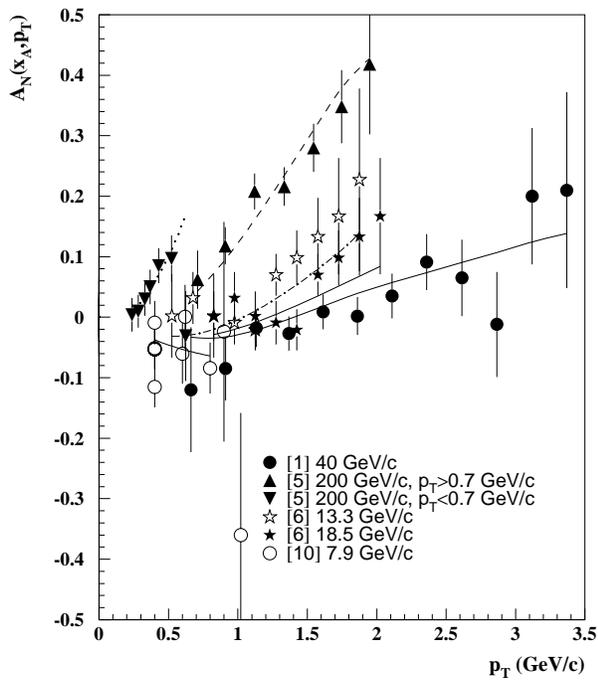
Fig. 1. A_N vs p_T for the π^+-production by polarized protons. The curves correspond to a fit by eqs. (6-10) with the parameters given in Table 1.
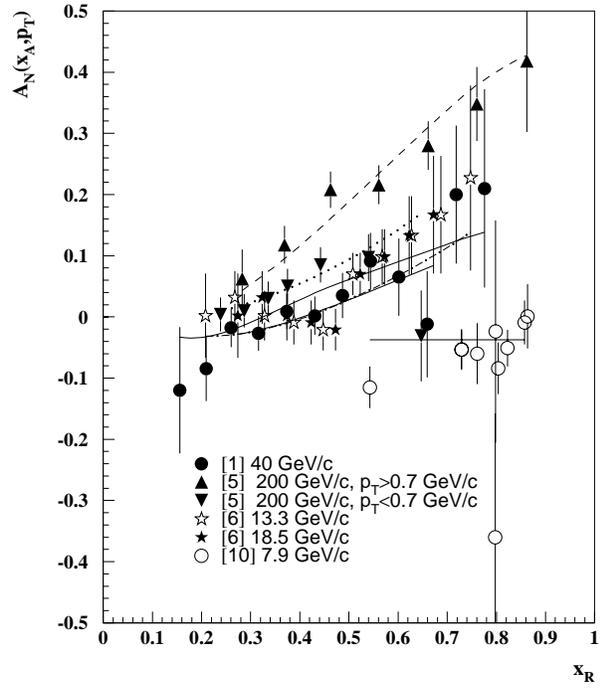
Fig. 2. A_N vs x_R for the π^+-production by polarized protons. The curves correspond to a fit by eqs. (6-10) with the parameters given in Table 1.

Fig. 3. A_N vs x_A for the π^+ production by polarized protons. The curves correspond to a fit by eqs. (6-10) with the parameters given in Table 1.

3
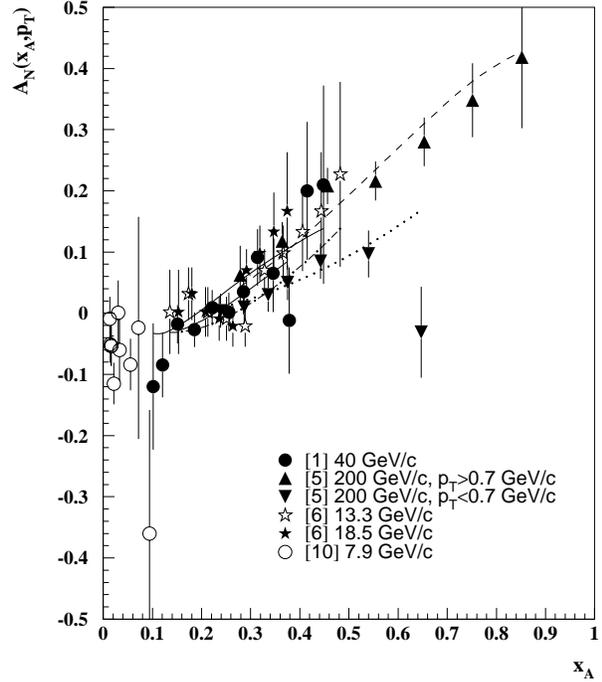
Asymmetry of π^+-production in $p\uparrow p$ collisions [1,5,6,10] is shown in Figs. 1,2 and 3 as a function of p_T, x_R, and x_A, respectively. The highest p_T (~ 3.5 GeV/c) is reached in [1], while the highest energy ($\sqrt{s} = 19.43$ GeV) in [5]. As is seen in Figs. 1 and 2, there is no scaling behavior of asymmetry as a function of p_T or x_R. Experiments, performed in forward, central and backward regions have asymmetry, decreasing from forward to backward region, with central region in the middle. Asymmetry, as a function of x_A, shows in Fig. 3 approximate scaling behavior for all three regions, mentioned above. Only the subset of data [5] with $p_T < 0.7$ GeV/c is below general trend, in agreement with the feature (d) above. Dependence of the asymmetry on x_A is close to a linear one in agreement with the feature (a) above. A simple expression, which takes into account all the features (a-e) can be used to fit the data shown in Fig. 3:

$$A_{N1} = F(p_T) \cdot \begin{cases} a_1 \sin(a_7(x_A - x_0)) + a_6/s, & \text{if } x_A \geq a_4; \\ a_1 \sin(a_7((a_4 - x_0) + a_5(x_A - a_4))) + a_6/s, & \text{otherwise;} \end{cases} \quad (6)$$

where $x_0 = a_2$ is a constant. Function $F(p_T)$ takes into account the above features (d) and (e) and has a correct asymptotic at high p_T, where the QCD predicts the vanishing of asymmetry [11]

$$F(p_T) = 2p_T a_3/(a_3^2 + p_T^2), \quad (7)$$

where p_T is measured in GeV/c and $a_1 - a_6$ are free fit parameters. The exact shape of $F(p_T)$ should be measured in future experiments. Parameters a_4, a_5 and a_6 are equal to zero, and $a_7 = 1$ for π^+-meson production reaction. They are introduced for other reactions, considered below, to take into account possible nonlinearity and non-asymptotic contribution to asymmetry. Point $x_A = x_0$ may be interpreted as a point where the relative phase of two helicity amplitudes (spin-flip and spin-nonflip) passes zero and, perhaps, changes its sign [7].

Along with the experiments presented in Figs. 1-3, there is an experiment with very thorough measurements of asymmetry at 11.75 GeV/c [13]. The measurements have been performed for a set of fixed secondary momenta, corresponding to fixed x_A values, and for each x_A as a function of angle or p_T. The data are presented in Figs. 4 and 5, as a function of x_A and p_T, respectively. As is seen from Figs. 4 and 5, only the points corresponding to the highest available p_T, which are about 1 GeV/c, are close to the scaling function (6) and to the experimental points shown in Fig. 3 for higher energies. Dependence of A_N on p_T is very different from the corresponding behavior at higher energies, shown in Fig. 1. To understand this difference of data [13] from the rest of the data, we have to assume that an additional contribution to asymmetry exists at 11.75 GeV/c ($\sqrt{s} = 4.898$ GeV) and low p_T. This additional contribution to asymmetry is approximated by the expression

$$A_{N0} = \left(b_1 \tanh(b_2(p_T - b_7)) \sin(b_8 x_A^{b_4}) + b_5 + b_6 x_A\right) F_0(p_T), \quad (8)$$

where function $F_0(p_T)$ suppresses asymmetry at low p_T

$$F_0(p_T) = 2p_T^2/(b_3^2 + p_T^2), \quad (9)$$

and $b_1 - b_8$ are free parameters.

4

Fit of a combined data set, which includes the data, presented in Figs. 3 and 4, requires additional assumption that the A_{N0} contribution decreases with energy, and the total asymmetry is

$$A_N = A_{N1} + A_{N0} \times (4.898/\sqrt{s})^{b_9}, \tag{10}$$

where b_9 is a free parameter.

The results of the combined data set fit are presented in Figs. 3 and 4 (corresponding curves) and in Table 1 (fit parameters). Two subsets of the combined data are shown in separate figures to give a clearer a representation of 117 data points. Parameter a_7 was fixed since the data show a linear dependence on x_A and the experimental accuracy is not sufficient to get a_1 and a_7 values separately. In all the fits below it is assumed that $a_7 = 1$, unless otherwise specified. The agreement between the fitting curves and the data is rather good. The analysis has shown that the contribution of A_{N0} term to (10) is small (≤ 0.08) for the experiments presented in Fig. 3. The term A_{N1} is, on the other hand, significant (≤ 0.3) for a kinematic region of the experiment [13], presented in Figs. 4 and 5.

<u>Table 1.</u> Fit parameters of eqs. (6)-(10) for π^+-mesons.

a_1	a_2	a_3	a_6
0.69 ±0.08	0.170±0.046	2.0 ±0.4	0.00
a_7	b_1	b_2	b_3
1.00	0.148±0.029	8.6 ±2.3	0.35 ±0.07
b_4	b_5	b_6	b_7
4.8 ±1.0	0.004 ±0.015	-0.148±0.041	0.646±0.016
b_8	b_9	N points	χ^2
5.6 ±2.6	2.0±1.9	117	114.4

The ratio of experimental asymmetry and $F(p_T)$, which is expected to be a function of x_A only, with a possible small dependence on $\sqrt{s}$, is shown in Fig. 6. The data from [13] are presented in Fig. 6 by two subsets, corresponding to $0.8 \leq p_T \leq 0.9$ GeV/c and $0.9 \leq p_T \leq 1.2$ GeV/c, respectively. All the experimental points in Fig. 6 are consistent with the simple function of x_A

$$A_N/F(p_T) = a_1 \cdot \sin(a_7(x_A - x_0)), \tag{11}$$

that confirms scaling behavior and factorization of p_T and x_A dependencies, assumed in (6) at high p_T and beam energy.
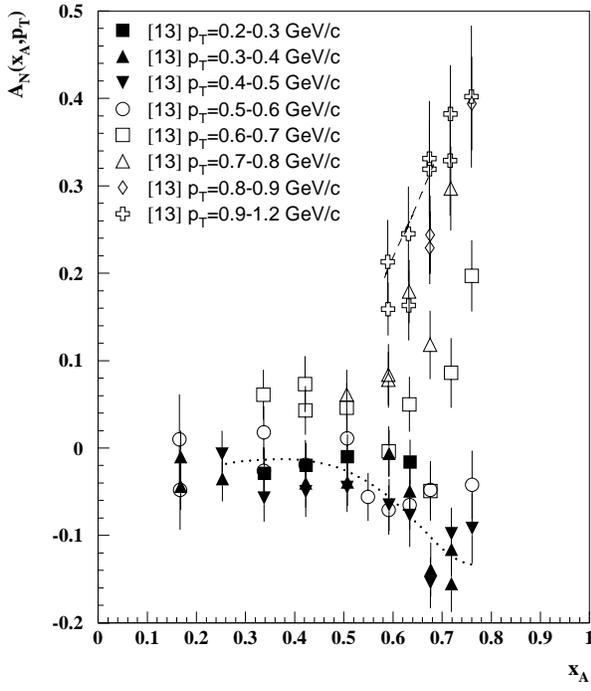
Fig. 4. A_N vs x_A for the π^+ production by polarized 11.75 GeV/c protons [13]. Dotted and dashed curves correspond to a fit by eqs. (6-10) for the regions $0.4 \leq p_T \leq 0.5$ and $0.9 \leq p_T \leq 1.2$ GeV/c, respectively.
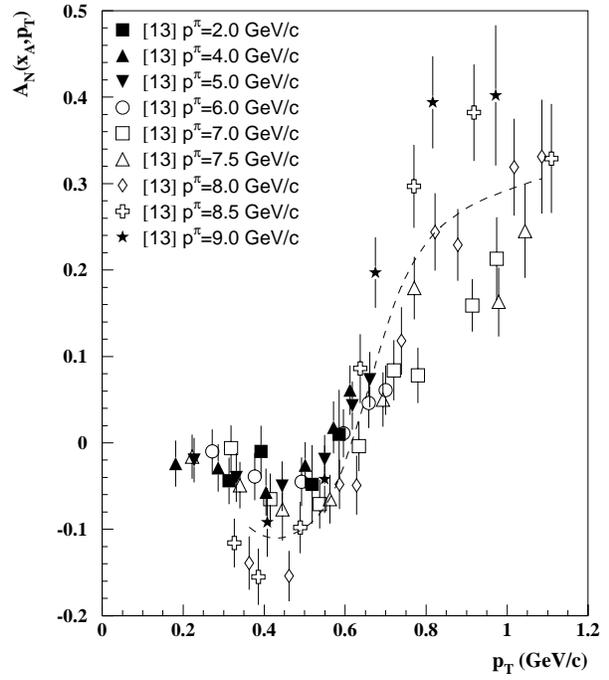
Fig. 5. A_N vs p_T for the π^+ production by polarized 11.75 GeV/c protons [13]. The curve corresponds to a fit by eqs. (6-10) for the $p^\pi = 8$ GeV/c.
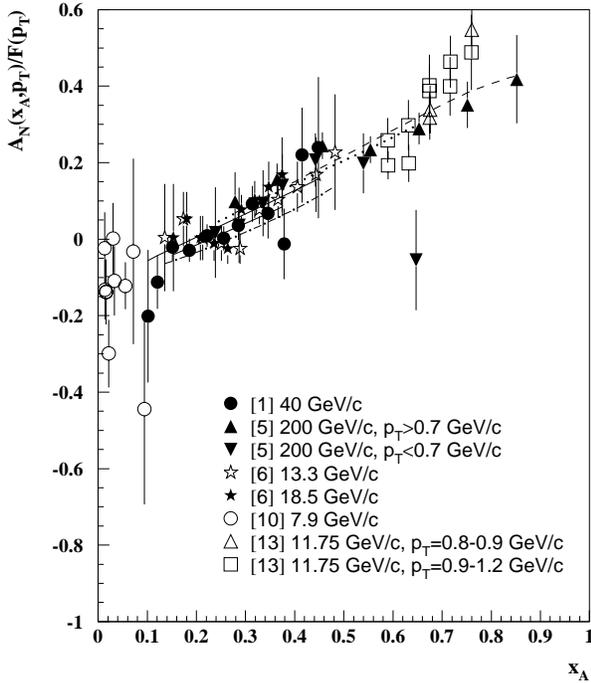
Fig. 6. The ratio $A_N/F(p_T)$ vs x_A for the π^+ production by polarized protons. The curves correspond to a fit by eqs. (6-10) with the parameters given in Table 1.

6

The results of the fit (10) show that the data sample [13] can be compatible with the rest of the data assuming that the additional contribution (8) is significant only at low beam energy and p_T. The physical nature of this contribution, which is negative at p_T near 0.4 GeV/c even at high x_A, is not completely clear. It could be a resonance contribution [15,11], or something else. Authors of [13] have assumed that the observed asymmetry is explained by the baryon exchange.

The existing experimental data at higher energies, presented in Fig. 3, are not very sensitive to the contribution (8), which is prominent at 11.75 GeV/c. A detailed experimental study of region $p_T \leq 1$ GeV/c at high energies and different production angles could help to understand its nature. The results of the fit by eq. (10) of 117 data points shown in Figs. 3 and 4, using a different definition of scaling variable (2) - (5) are presented in Table 2. Only parameters $a_1 - a_3$ are free. All other parameters are the same as in Table 1. The difference in χ^2 is not very significant, with a small preference for eqs. (2), (4) and (5) variables.

Table 2. Fit parameters of eq. (6) for π^+-mesons. Different definitions of the scaling variable x_A are used for comparison (eqs. (2)-(5)).

eq.	a_1	a_2	a_3	χ^2
(2)	0.69 ±0.08	0.169±0.047	2.0 ±0.4	114.4
(3)	0.74 ±0.07	0.166±0.013	2.2 ±0.3	120.4
(4)	0.69 ±0.07	0.167±0.013	2.1 ±0.3	114.6
(5)	0.68 ±0.06	0.170±0.013	2.0 ±0.2	114.2

The error ($\epsilon = 0.025$), added in quadrature to each data point during the fitting procedure, has not changed the fit parameters significantly, but decreased χ^2 by about a factor of two up to a level of about unity per degree of freedom. Errors, shown in Figures, representing experimental data, also include this additional error.

2. Asymmetry for $p^\uparrow p \to \pi^- + X$-reaction

Asymmetry for π^--meson production by polarized protons [1,5,6,10] is shown in Fig. 7 as a function of x_A. As with π^+-mesons, we observe an approximate scaling in A_N vs x_A. Selection of data with $p_T \geq 0.8$ GeV/c and $E^{BEAM} \geq 40$ GeV leads to a good agreement between two experiments [1,5] which implies their scaling behavior. Experiment [13] reveals quite different x_A and p_T-dependencies at 11.75 GeV/c, in Figs. 8 and 9, respectively. As with π^+, the greatest deviation from the scaling behavior is for low p_T. At $p_T = 0.15$ GeV/c asymmetry is very large and positive contrary to the large energy behavior, where it is negative. The possible nature of this low energy asymmetry is probably the same as that discussed above for π^+-mesons, and its approximation is given by eqs. (6) - (10).

7
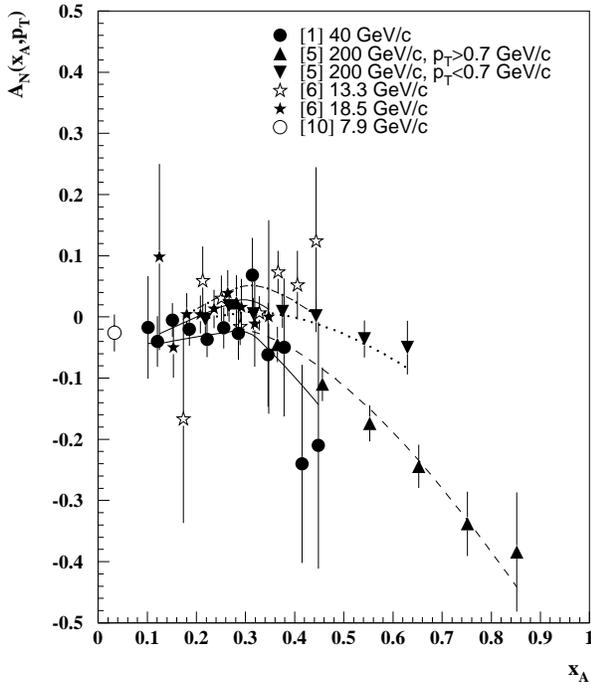
Fig. 7. A_N vs x_A for the π^--production by polarized protons. The curves correspond to a fit by eqs. (6-10) with the parameters given in Table 2.
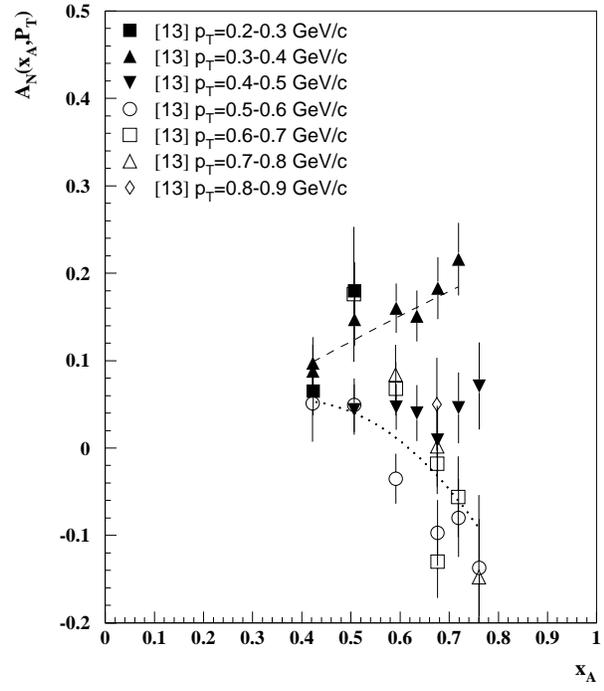
Fig. 8. A_N vs x_A for the π^--production by polarized 11.75 GeV/c protons [13]. The dashed and dotted curves correspond to a fit by eq. (6-10) for the regions $0.3 \leq p_T \leq 0.4$ and $0.5 \leq p_T \leq 0.6$ GeV/c, respectively.
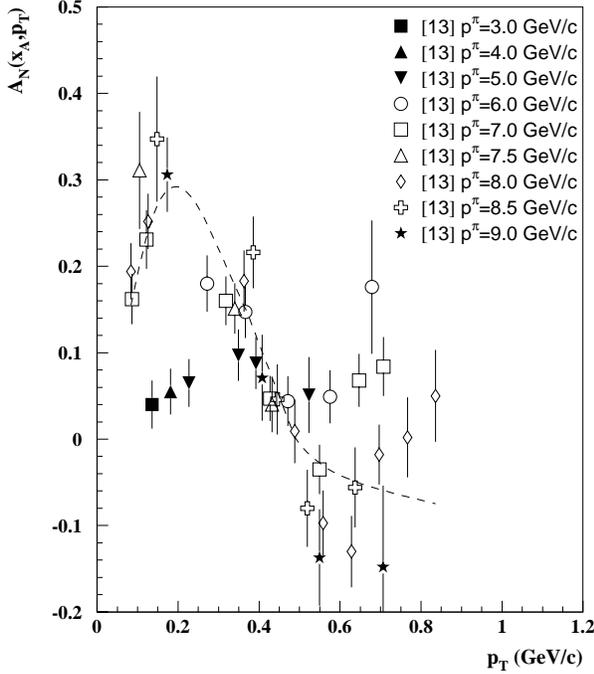
Fig. 9. A_N vs p_T for the π^--production by polarized 11.75 GeV/c protons [13]. The curve corresponds to a fit by eqs. (6-10) for the $p^\pi = 8$ GeV/c.

8

The difference is that parameters a_4 and a_6 are now not zero, while $a_5 = 0$. Fit parameters of the combined data sample, shown in Figs. 7 and 8, are presented in Table 3. Some of the parameters could not be well determined from the existing data and were fixed ($a_3 = 4.8$, $a_7 = 1$) during the fitting procedure. The role of energy-dependent term (a_6/s) is more significant for π^-, than for π^+-mesons. Possible explanation can be related to resonance contribution [15]. Asymmetry in low $x_A \leq 0.3$ -region is close to zero in agreement with an expected large gluon contribution [11].

<u>Table 3.</u> Fit parameters of eqs. (6)-(10) for π^--mesons.

a_1	a_2	a_3	a_4
-0.96 ±0.20	0.185±0.075	4.80	0.303±0.045
a_6	b_1	b_2	b_3
3.8 ±1.8	-0.345 ±0.089	8.0 ±2.8	0.115±0.024
b_4	b_5	b_6	b_7
3.1 ±0.5	-0.047 ±0.018	0.256±0.052	0.344±0.028
b_8	b_9	N points	χ^2
1.12±0.27	0.76 ±0.39	84	89.5

3. Asymmetry for $p^\uparrow p \to p + X$-reaction

Asymmetry for proton production has been measured at 6 different beam energies, from 6 up to 40 GeV [1,6,13,10,14]. It is shown in Fig. 10 as a function of x_A. The absolute value of A_N is small (≤ 0.1) and with the present day accuracy A_N is compatible with the approximate x_A-scaling, especially, when taking into account possible systematic errors of the order of 0.02. Nevertheless, the data fitting function (eq. (6)) is modified to give a better approximation. In particular, the fit approximates the data better if a fitting function is not suppressed at high p_T, as is the case with eq. (7). Non-asymptotic contribution to A_N at low energies is more significant for protons than for π^--mesons and was approximated by $a_6/s^{0.5}$ term. Eqs. (12) and (13) are used to fit the proton production asymmetry

$$A_N = F_p(p_T)(a_1 \sin(a_7(x_A - x_0)) + a_6/s^{0.5}), \qquad (12)$$

where

$$F_p(p_T) = 1 - \exp(-p_T/a_3). \qquad (13)$$

Extra error $\epsilon = 0.015$ is added to each data point. Comparison of fit parameters for different definitions of x_A, given by eqs. (2)-(5), is shown in Table 4. The best χ^2 is reached if x_A is given by eq. (4). Asymmetry slightly rises with x_A increase and changes

its sign near $x_A = 0.5$ at energies around 10 GeV. Additional measurements of A_N for protons at high energies in the fragmentation region of polarized proton could help to clarify a possible energy dependence of the asymmetry.

Table 4.   Fit parameters of eqs. (12-13) for the protons and different definitions of the scaling variable x_A, eqs. (2) - (6). Parameters a_4 - a_5 are set equal to zero and $a_7 = 1$ during the fit.

eq.	a_1	a_2	a_3	a_6	χ^2 / points
(2)	0.116±0.011	0.81 ±0.15	0.184 ±0.006	0.216±0.080	120.9/ 150
(3)	0.117±0.012	0.90 ±0.13	0.186±0.007	0.316±0.078	125.6/ 150
(4)	0.117±0.011	0.82 ±0.14	0.187±0.006	0.230±0.080	118.6/ 150
(5)	0.117±0.011	0.83 ±0.14	0.187 ±0.006	0.236±0.079	119.4/ 150
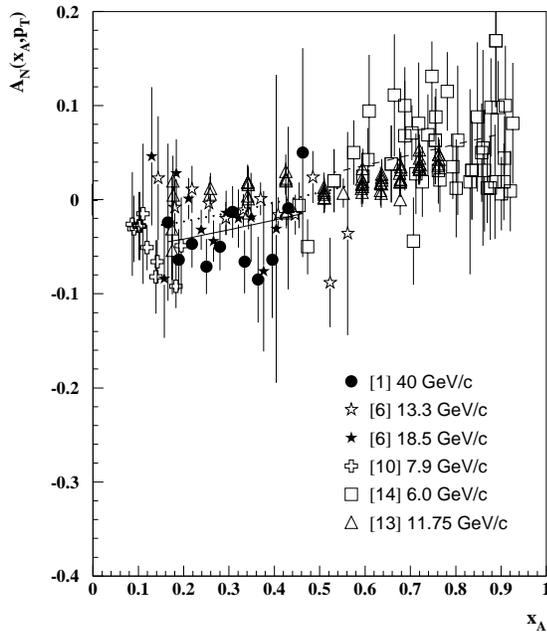
Fig. 10. A_N vs x_A for the proton production by polarized protons. The solid fitting curve corresponds to the 40 GeV/c data [1]. The dotted curve corresponds to the 13.3 GeV/c data [6]. The dashed curve corresponds to the 6 GeV/c data [14].

4. Asymmetries for π^0, K^+, K^- and $\bar{p}$ production by polarized protons

Asymmetry for π^0-meson production in $p^{\uparrow}p$ collisions has been measured at 24, 185 and 200 GeV/c [9,24,4,3,25]. The data are shown in Fig. 11 as a function of x_A. They are compatible with a simple linear dependence given by eq. (6). The fit parameters are shown in Table 5. A very large asymmetry observed at 24 GeV/c [9] probably results from statistical fluctuations. It is hard to expect A_N for π^0 greater than that for π^+ in the same kinematic area.

10

Table 5. Fit parameters of eq. (6) for the π^0, K^+, K^--mesons and $\bar{p}$. Parameters a_4 - a_5 are set equal to zero during the fit.

h_3	a_1	a_2	a_3	a_6	χ^2 / points
π^0	0.24 ±0.04	0.111±0.019	1.40±0.49	0	50.5 / 54
K^+	0.37 ±0.08	0.183±0.045	1.15±0.34	0	65.8 / 67
K^-	1.88 ±0.34	0.086±0.054	0.246±0.070	-13.5 ±4.2	24.2 / 28
$\bar{p}$	0.6 ±1.0	0.16 ±0.12	1.00	0	15.6 / 11
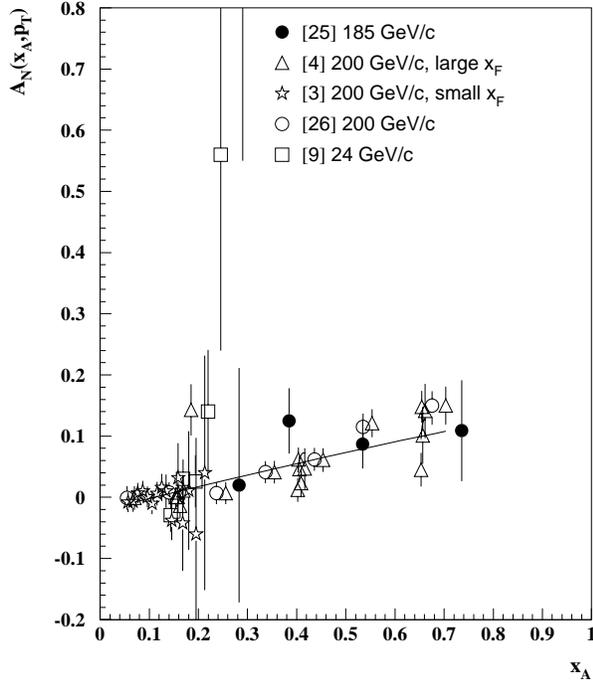
Fig. 11. A_N vs x_A for the π^0 production by polarized protons. The fitting curve corresponds to the 200 GeV/c data [4].
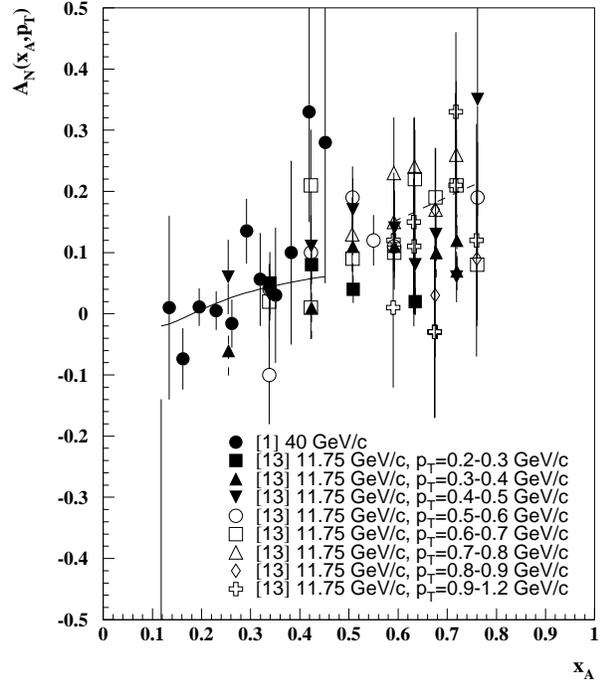
Fig. 12. A_N vs x_A for the K^+ production by polarized protons. The solid fitting curve corresponds to the 40 GeV/c data [1], and the dashed curve corresponds to the 11.75 GeV/c data [13] and $0.5 \leq p_T \leq 0.6$ GeV/c.

K^+-meson production asymmetry in $p^{\uparrow}p$-collisions has been measured in two experiments [1,13] at 40 and 11.75 GeV/c, respectively. It is shown in Fig. 12 as a function of x_A. The dependence of A_N on kinematic variables was approximated by eq. (6) with $a_4 = 0$ and $a_6 = 0$, because statistical accuracy of the data is limited. The fit parameters are presented in Table 5. The experimental data are compatible with the x_A-scaling (6), but the existing accuracy is not enough to exclude nonzero parameters a_4 and a_6.

Asymmetry for K^--mesons production has been measured at 40 and 11.75 GeV/c [1,13]. It was fitted by eq. (6) with a_6, as a free parameter and $a_4 = 0$. The energy dependent term a_6/s significantly improves the fit for K^-, contrary to the K^+ case. The parameters of the fit are shown in Table 5. The ratio $A_N/F(p_T)$ is shown in Fig. 13 vs x_A, where shift of data points due to a_6/s term is clearly seen. The parameter a_3 for K^--meson, which has no valence quarks common for colliding protons, is much smaller than in the case with K^+-meson and is close to the estimation of Ref. [11]. Contrary to $\pi^\pm$-mesons, $K^\pm$-mesons do not show any unusual behavior at 11.75 GeV/c which requires an additional contribution to the asymmetry similar to that given by eq. (8).

The asymmetry for antiprotons has been measured only at 40 GeV/c and a single fixed laboratory angle [1]. So, it is not possible to determine parameter a_3, which was fixed at 1 GeV/c during the fit of the data by eq. (6). The fit parameters are presented in Table 5 and A_N vs x_A is shown in Fig. 14.

Additional measurements are required for K^+, K^--mesons, and antiprotons at different energies and production angles to check the x_A-scaling and determine the parameters of eq. (6).
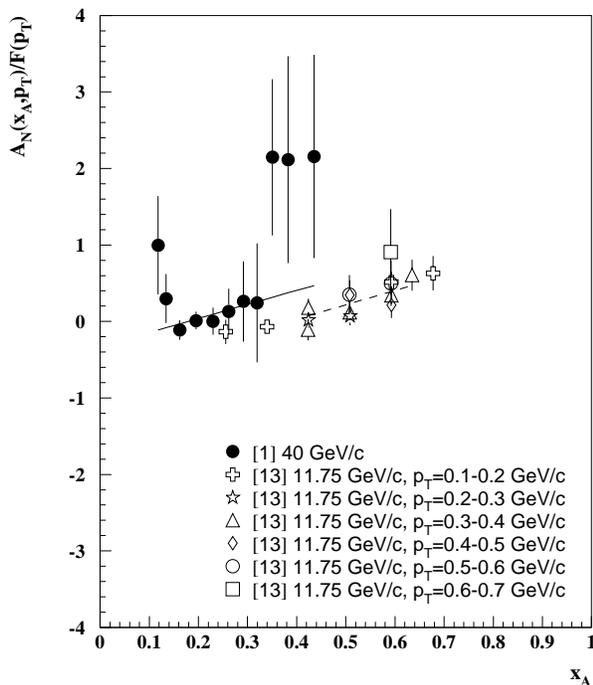
Fig. 13. The ratio $A_N/F(p_T)$ vs x_A for the K^--production by polarized protons. The solid fitting curve corresponds to the data [1], and the dashed curve corresponds to the data [13] and region $0.3 \leq p_T \leq 0.4$ GeV/c.
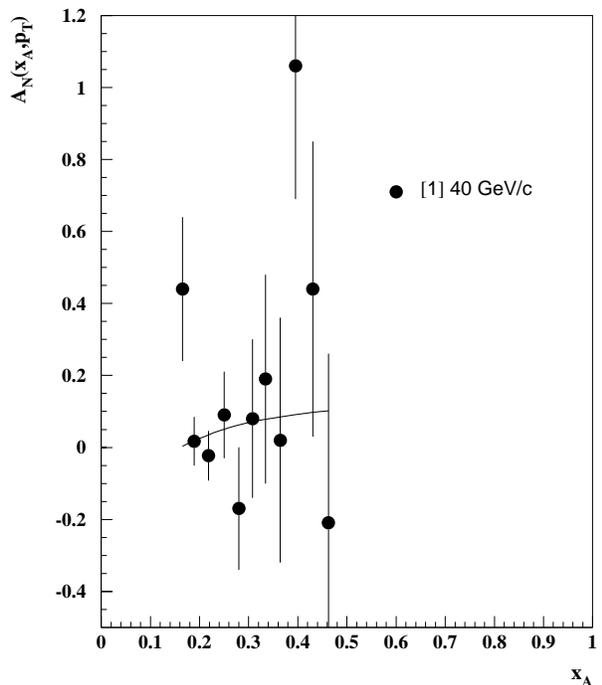
Fig. 14. A_N vs x_A for antiproton production by polarized protons. The curve corresponds to a fit by eq. (6) with the parameters given in Table 5.

12

5. Asymmetries for Λ, K_S^0, η production by polarized protons

Asymmetry for the Λ-hyperon production has been measured at 13.3, 18.5 and 200 GeV/c [16,17]. It is shown as a function of x_A in Fig. 15 along with fitting curves (eq. (6)). The fit parameters for different x_A definitions are presented in Table 6. As is seen from Fig. 15, A_N can be described at different energies by the same function of the scaling variable x_A at a present value of experimental errors. A_N is near zero for the region $0.2 \leq x_A \leq 0.6$ and is negative for the x_A above 0.6. The best χ^2 is attained with x_A defined by eq. (3).

<u>Table 6.</u> Fit parameters of eq. (6) for the Λ and different definitions of scaling variable x_A, eqs. (2) -(5).

eq.	a_1	a_2	a_3	a_4	a_5	χ^2 / points
(2)	-0.52 $\pm$0.15	0.557$\pm$0.036	0.66 $\pm$0.36	0.563$\pm$0.035	-0.111$\pm$0.096	39.4 / 49
(3)	-0.72 $\pm$0.38	0.539$\pm$0.021	1.6 $\pm$1.3	0.527$\pm$0.024	-0.158 $\pm$ 0.073	24.3 / 49
(4)	-0.54 $\pm$0.15	0.560$\pm$0.034	0.69 $\pm$0.37	0.564$\pm$0.033	-0.109$\pm$0.091	38.3 / 49
(5)	-0.53 $\pm$0.15	0.559$\pm$0.034	0.68 $\pm$0.37	0.564$\pm$0.034	-0.109$\pm$0.091	38.5 / 49

Fig. 15. A_N vs x_A for the Λ production by polarized protons. The solid fitting curve corresponds to the 18.5 GeV/c data [16], and the dashed curve corresponds to the 200 GeV/c data [17].
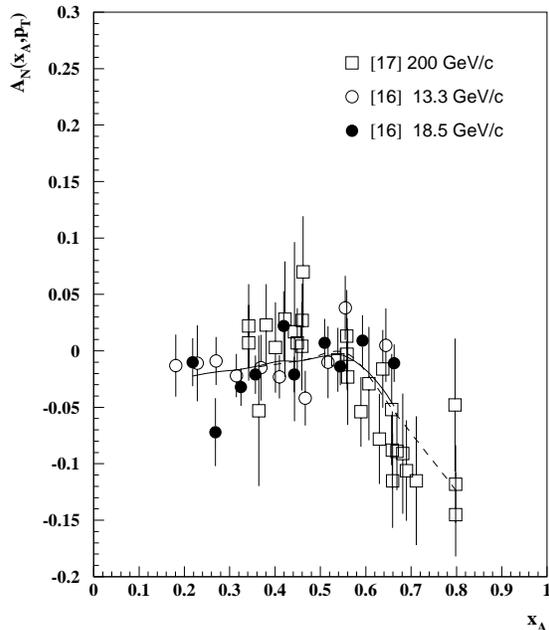
Measurements of A_N for the K_S^0-mesons have been performed at 13.3 and 18.5 GeV in the central region only [16,18]. A_N as a function of x_A is shown in Fig. 16 along with a fitting curve given by eq. (6). The fit parameters are presented in Table 7. The data are compatible with the x_A-scaling, but additional measurements are desirable to check it at different energies and in the fragmentation region.

13

Asymmetry for the η-meson production in $p^\uparrow p$ collisions has been measured at 200 GeV/c [26]. It is shown in Fig. 17 along with the fitting curve, eq. (6). The fit parameters are shown in Table 7. Since the measurement has been performed at a fixed angle, parameter a_3 was fixed during the fit.

Table 7.   Fit parameters of eq. (6) for the K_S^0 and η-mesons.

h_3	a_1	a_2	a_3	χ^2 / points
K_S^0	-0.143±0.095	-0.49 ±0.50	0.79 ±0.49	4.4 / 16
η	1.00 ±0.36	0.323±0.048	1.00	0.0 / 4
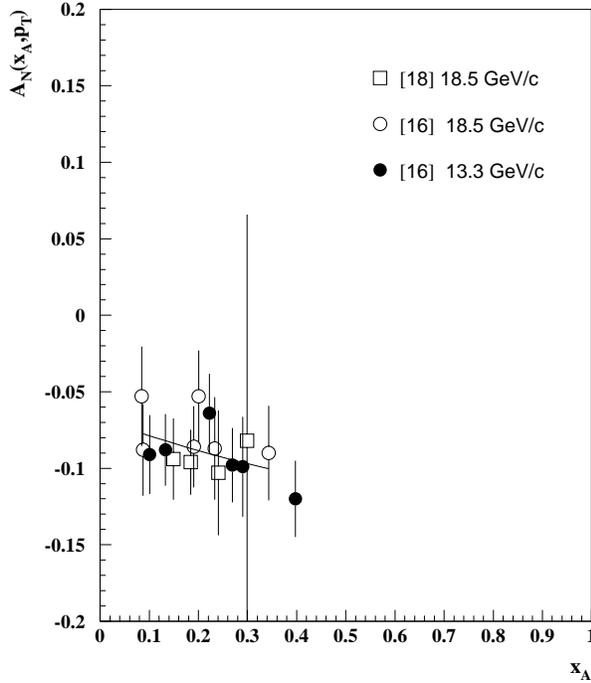
Fig. 16. A_N vs x_A for the K_S^0 production by polarized protons. The fitting curve corresponds to the 18.5 GeV/c data [16].
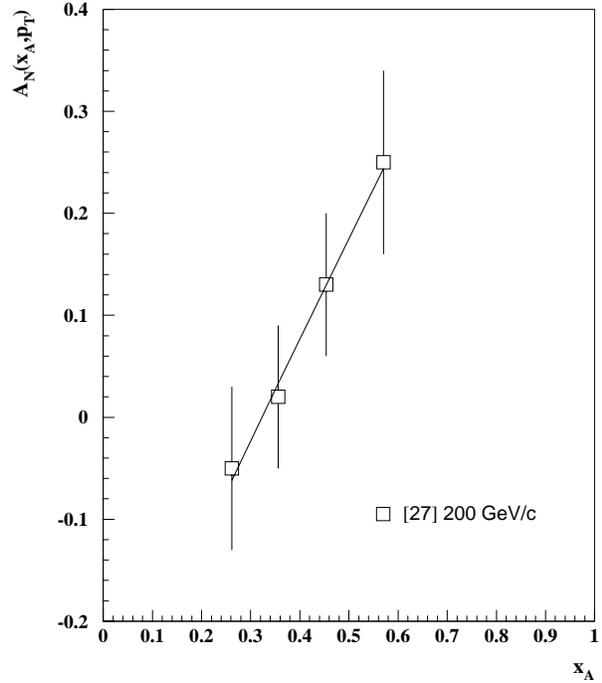
Fig. 17. A_N vs x_A for the η production by polarized protons. The curve corresponds to a fit (6) with the parameters given in Table 7.

6. Asymmetries for the π^0 and η-production in $\pi^- p^\uparrow$-collisions

Asymmetry measurements for the π^0 and η-meson production have been performed at 40 GeV/c in the central region [23] and in the fragmentation region of π^--meson [27]. The data for the π^0-mesons are shown in Fig. 18 along with the fitting curve (eq. (6)). The

14

dashed curve shows prediction of eq. (6) for region $0.03 \leq x_A \leq 0.1$ and $p_T = 1$ GeV/c, where no data exist and a local minimum of A_N is expected from the fit. Dash-dot curve shows prediction for region $p_T = 2$ GeV/c and $x_A \geq 0.3$, where a local maximum of A_N is expected near $x_A = 0.3$, and a local minimum is expected near $x_A = 0.5$. The use of $\sin(a_7(x_A - x_0))$ in eq. (6) allows one to satisfy constrain $|A_N| \leq 1$. The fit parameters are shown in Table 8.

Table 8. Fit parameters of eq. (6) for the π^0- and η-meson production in $\pi^- p$-collisions.

h_3	a_1	a_2	a_3	a_4	a_5	a_7	χ^2 / points
π^0	1.00 ±0.40	0.131±0.008	0.3±1.3	0.078±0.062	-0.8±1.7	12.0	15.2 / 20
η	1.00 ±0.49	0.154±0.016	1.0	0.0	0.0	12.5	0.2 / 3
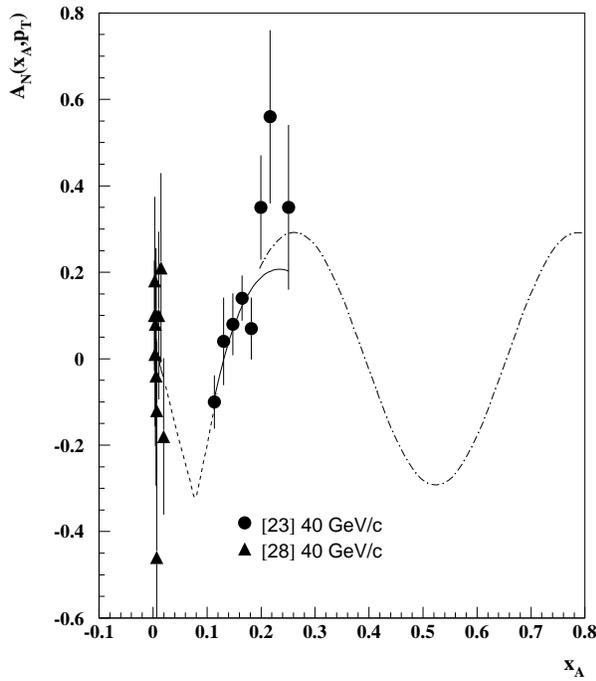
Fig. 18. A_N vs x_A for the π^0 production in $\pi^- p^\uparrow$-collisions. The solid curve corresponds to a fit by eq.(6) with the parameters given in Table 8. The dashed curve corresponds to an extrapolation of the fit (6) for the region $p_T = 1$ GeV/c and $0.03 \leq x_A \leq 0.1$. The dash-dot curve corresponds to an extrapolation of the fit (6) for the region $p_T = 2$ GeV/c and $x_A \geq 0.3$.
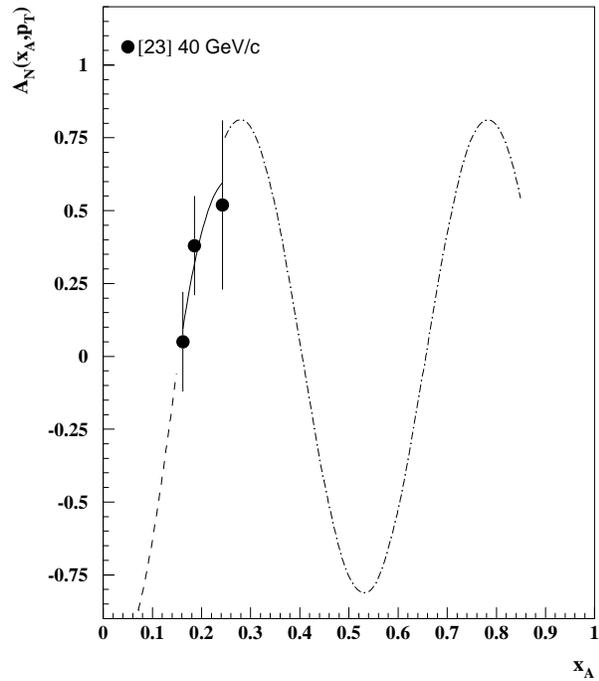
Fig. 19. A_N vs x_A for the η-production in $\pi^- p^\uparrow$-collisions. The solid curve corresponds to a fit by eq. (6) with the parameters given in Table 8. The dashed curve corresponds to an extrapolation of the fit (6) for the region $p_T = 1$ GeV/c and $x_A \leq 0.15$. The dash-dot curve corresponds to an extrapolation of the fit (6) for the region $p_T = 2$ GeV/c and $x_A \geq 0.3$.

Asymmetry vs x_A for the η-meson production is shown in Fig. 19. Since only a few experimental points have been measured, some of the parameters of eq. (6) were fixed (see Table 8). Predictions for region $x_A \leq 0.15$ and $p_T = 1$ GeV/c are shown by the dashed curve, and predictions for region $x_A \geq 0.3$ and $p_T = 2$ GeV/c are shown in Fig. 19 by the dash-dot curve. As in the case of π^0-production, a local maximum of A_N is expected (near $x_A = 0.3$). Also a local minimum of A_N is expected near $x_A = 0.5$. For both π^0 and η-meson production by π^- beam, the dependence on x_A looks very similar having a fast rise in the range $0.15 \leq x_A \leq 0.3$. This behavior is very different from the x_A-dependence in $p^\uparrow p$-collisions, where the rise of A_N with x_A is not so dramatic and $sin(x)$ function in eq. (6) is not very important at the present level of accuracy.

7. Asymmetries for the $\pi^\pm$, π^0 and η production in $\bar{p}^\uparrow p$-collisions

A_N for the $\pi^\pm$-meson production in the fragmentation region of polarized antiprotons has been measured at 200 GeV/c [2]. It is shown in Figs. 20 and 21, as a function of x_A, for the π^+ and π^-, respectively. Fit parameters are presented in Table 9. Parameter a_3 has been fixed due to limited statistics.
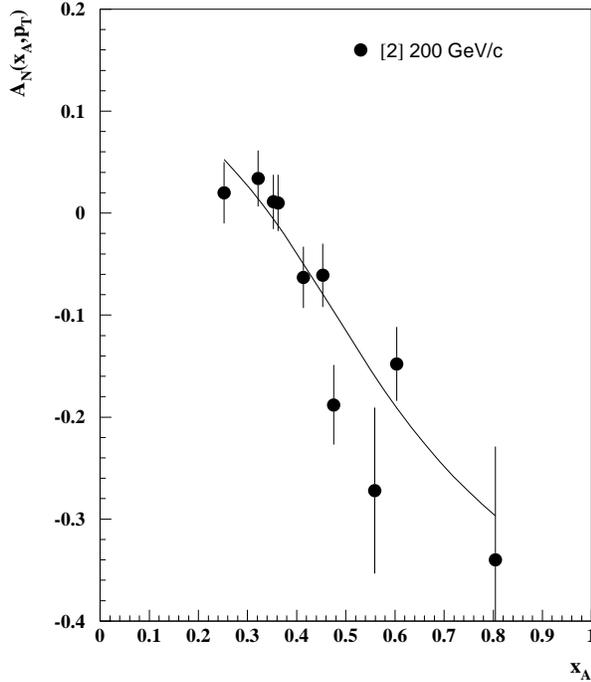
Fig. 20. A_N vs x_A for the π^+ production in $\bar{p}^\uparrow p$-collisions. The curve corresponds to a fit by eq. (6) with the parameters given in Table 9.
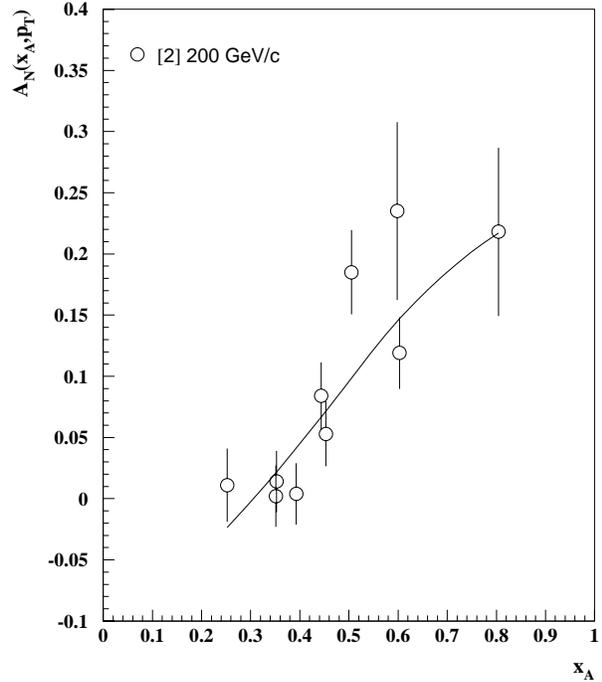
Fig. 21. A_N vs x_A for the π^--production in $\bar{p}^\uparrow p$-collisions. The curve corresponds to a fit by eq. (6) with the parameters given in Table 9.

A_N for the π^0-meson production in $\bar{p}^\uparrow p$-collisions has been measured at 200 GeV/c in the central region [3] and the fragmentation region [25] of polarized antiprotons. It is shown as a function of x_A along with fitting curve (eq.(6)) in Fig. 22. The fit parameters are shown in Table 9.

A_N for the η meson production has been measured just in a few points at 200 GeV/c [26]. Fit parameters are shown in Table 9.

It is easy to notice that a_2-parameter for the $\pi^\pm$ and η-meson production by polarized antiprotons is larger by about 0.15 compared to the case of polarized proton beam. On the other hand, it is the smallest for the case of $\pi^- p^\uparrow$-collisions.
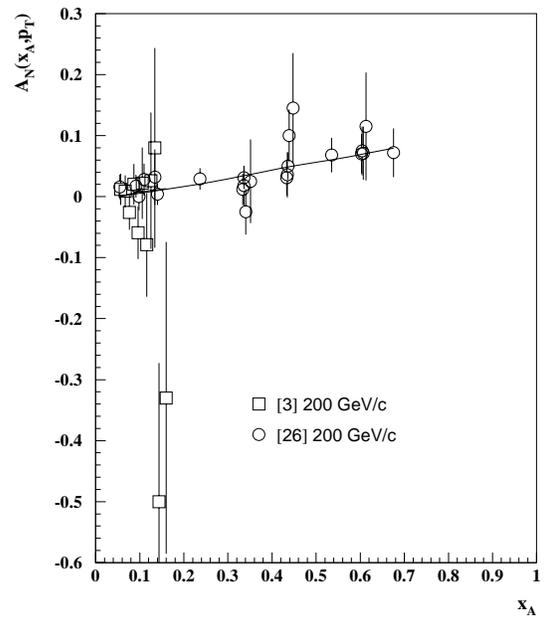
Fig. 22. A_N vs x_A for the π^0 production in $\bar{p}^\uparrow p$-collisions. The fitting curve corresponds to the 200 GeV/c data [28].

<u>Table 9.</u> Fit parameters of eq. (6) for the $\pi^\pm$, π^0, and η-meson production in $\bar{p}p$-collisions.

h_3	a_1	a_2	a_3	a_7	χ^2 / points
π^+	-0.32 ±0.20	0.344±0.020	1.0	2.8±2.1	10.4 / 10
π^-	0.23 ±0.10	0.309±0.035	1.0	2.8±1.8	10.1 / 10
π^0	0.15 ±0.07	0.050±0.061	1.5 ±1.3	1.0	21.1 / 34
η	-1.1 ±0.9	0.468±0.075	1.0	1.0	0.9 / 3

8. Discussion

In this section we will try to understand the observed the x_A-scaling, which is approximated by eqs. (6) - (10), in the framework of ideas of existing models. We begin our discussion of the results with a set of rules which reproduce the known features of the data.

Single-spin asymmetry for hadron production, as well as hyperon polarization in inclusive reactions are proportional to an imaginary part of the product of spin-flip and spin-nonflip amplitudes

$$A_N \propto Im(f_{snf}f_{sf}^*) = |f_{snf}||f_{sf}|sin(\Delta\phi), \qquad (14)$$

17

where $\Delta\phi$ is a phase difference of the corresponding amplitudes [11,23]. Zero of $\Delta\phi$ means $A_N = 0$, so we may suggest that at $x_A = x_0$ phase difference $\Delta\phi = 0$ in case of π^+-meson production at high energy and p_T.

The sign of asymmetry at a quark level is given by the rule: Quark with spin *up* prefers scattering to the *left*, and vice versa. Such result is easy to get by taking into account the interaction of quark chromomagnetic momentum with chromomagnetic field, arising after the collision during hadronization [11,12].

The effect of recombination of partons in the proton while they transfer into an outgoing hadron may be different depending on whether they are accelerated (as with slow sea quarks) or decelerated (as with fast valence quarks). Slow partons mostly recombine with their spin downwards in the scattering plane while fast partons recombine with their spin upward [19].

Existence of the x_0 point in eq. (6), where the asymmetry changes its sign, can be explained by the same arguments which are used to explain x_F-dependence of Λ-hyperon polarization in the SU(6) based parton recombination model [19]. Following the same arguments we can say that the asymmetry for the Λ-production is proportional to Δp-change in the momentum of sea s-quark:

$$\Delta p_S \propto 1/3(x_F - 3x_S), \tag{15}$$

where $x_S \approx 0.1$ is a fraction of proton momentum, which carries sea s-quark. Substituting x_F by x_A, we get the expression similar to eq. (6) with $x_0 = 3x_S$ about 0.3, which agrees qualitatively with the experimental data (see Fig. 15) for production asymmetry of Λ-hyperon, which is near zero for $0.2 \leq x_A \leq 0.6$. The only difference is the absence of $sin(x)$ function in eq. (15), which is not very essential since the asymmetry is small.

In case of π^+, K^+-meson production we can apply similar arguments. In this case Δp for sea quark ($\bar{d}$ or $\bar{s}$) is

$$\Delta p_{SEA} \propto 1/2(x_F - 2x_{SEA}), \tag{16}$$

and we again have the expression similar to eq. (6) with $x_0 = 2x_{SEA}$ about 0.2 in agreement with the experimental data (see Table 1). An accelerated sea quark has spin downwards and recombines with valence spin upward u-quark from polarized proton, producing π^+ or K^+-meson preferably to the left, which means positive asymmetry. At $x_A \leq x_0$, acceleration changes for deceleration, which reverses the sea quark spin direction and the asymmetry sign.

A dynamical reason for the above spin-momentum correlation is explained in [19] by the effect of Thomas precession [20]. Another explanation of spin-momentum correlation comes from a picture of color flux tube, which emerges after the collision between an outgoing quark and the rest of hadronic system [11,21].

Asymmetry of π^+-production by polarized protons is determined by a product of elementary subprocess asymmetry (A_q for polarized quark production), polarization of this quark (P_q), and a dilution factor due to the presence of other contributions, not related with valence quark fragmentation [11]

$$A_N = A_q P_q \sigma(q)/(\sigma(q) + \sigma(g)). \tag{17}$$

18

Quark polarization according to SLAC [22] measurements is rising with a fraction of momentum carried by quark and in the first approximation can be taken as $P_q = x_A$, which is the generalization of $P_q = x_F$, assumed in [11]. As A_q, we take the expression

$$A_q = \delta p_T \cdot 2p_T/(m^2 + p_T^2), \tag{18}$$

where δp_T (~ 0.1 GeV/c) is an additional transverse momentum, which quark with spin upward acquires in the chromomagnetic field of the flux tube, and m^2 is some effective quark mass squared [11]. This expression for A_q is similar, in its functional form, to the lower order QCD calculations and gives A_N decreasing down to very small values at very high p_T. In our case A_q is proportional to $F(p_T)$, given by eq. (7). The resulting expression for the A_N is

$$A_N = \delta p_T \cdot x_A \cdot 2p_T/(m^2 + p_T^2)D(x_A), \tag{19}$$

where $D(x_A)$ is a dilution factor mentioned above. Eq. (19) is very similar to eq. (6) and its high energy limit (11) with $x_0 = 0$. The difference is in numerical values of parameters in eqs. (19) and (6). In our cases $\delta p_T = a_1 a_3 a_7 = 1.4$ GeV/c, and $m = a_3 = 2$ GeV, instead of $m = 0.33$ GeV in [11]. Parameters, which are much closer to those given in Table 1, have been estimated in [23] ($m = 2$ GeV).

Another argument in favor of asymmetry and phase difference between spin-flip and spin-nonflip amplitudes to be proportional to hadron energy is given in [23,29]. The reason is that probability of quark spin-flip in an external field is proportional to a quark mean range before its hadronization. Experimental estimate of the hadronization range indicates that it is proportional to the secondary hadron energy [30].

We may conclude that eq. (6), which describes scaling behavior of asymmetries, has a reasonable explanation of its major components in the framework of the existing models. Resuming the discussion above we may suggest that the observed x_A-scaling is due to the dependence of phase difference of spin-flip and spin-nonflip amplitudes at high p_T and energy on x_A only. This dependence for some hadrons $(\pi^+, \pi^0, K^\pm, K_S^0, \eta, \bar{p})$ has a very simple form:

$$\Delta\phi \propto a(x_A - x_0). \tag{20}$$

The x_A-dependence of asymmetries reflects in some models the corresponding dependence of constituent quark polarization in the polarized proton [31].

The p_T-dependence of asymmetry, given by eq. (7), reflects probably the ratio of spin-flip and spin-nonflip amplitudes [23]:

$$F(p_T) = 2p_T a_3/(a_3^2 + p_T^2) \propto \frac{|f_{snf}||f_{sf}|}{|f_{snf}|^2 + |f_{sf}|^2}. \tag{21}$$

Both suggestions are not rigorously proved, but they seem reasonable in view of the above arguments.

It is interesting to note that maximum of $F(p_T)$ takes place at approximately the same p_T, where the dip in elastic $p^\uparrow p$-scattering exists and where the interference maximum of spin-flip and spin-nonflip amplitudes takes place [32].

A more detailed comparison of different model predictions with scaling behavior of experimental asymmetry is the subject for a separate paper.

9. Scaling predictions for future experiments

The existence of the x_A-scaling is established from a limited set of data which cover only a restricted range of kinematic variables (p_T, x_A, and $\sqrt{s}$). The corresponding CM angles are concentrated mostly near 0°, 90°, and 180°. More detailed study of p_T, x_A, and energy dependence could clarify theoretical basis of the x_A-scaling and help in comparing it with various models.

Detailed predictions of A_N-dependence on x_A for π^+-production at different laboratory angles in $p^\uparrow p$-collisions at 40 GeV/c are shown in Fig. 23. This dependence is given by eqs. (6)-(10)with the parameters presented in Table 1. The measurements can be performed at the FODS-2 experimental setup in IHEP (Protvino) which uses 40 GeV/c polarized proton beam [1]. As is seen from Fig. 23, asymmetry is negative for the x_A near 0.08 and grows in an absolute value with the rise of laboratory angle. At $x_A = 0.19$ A_N is always equal to zero and can be used to check systematic errors in asymmetry measurements. The largest values of A_N are reached for laboratory angle near 70 mrad. At this angle the values of x_A and A_N could be larger than 0.8 and 0.4, respectively. At smaller angles and large x_A, asymmetry is smaller due to the decrease of p_T and the corresponding decrease of the function $F(p_T)$ (see eq. (7)).

The dependence of A_N for the π^+-production in $p^\uparrow p$-collisions at 40 GeV/c on p_T at several values of x_A is shown in Fig. 24. It is possible to measure not only the rise of A_N for $0 \le p_T \le 2$ GeV/c, but also its probable decrease at higher p_T even at 40 GeV beam energy. For the x_A values near 0.6, we can measure the shape of p_T-dependence up to 4 GeV/c. Much higher $p_T \le 10$ GeV/c can be reached at 200 GeV, where A_N could decrease significantly compared to its maximum value at p_T around 2 GeV/c.

Dependence of A_N for the π^+-production in $p^\uparrow p$-collisions on x_A at different beam energies and $p_T = 0.5$ GeV/c is shown in Fig. 25. The corresponding parameters are taken from Table 1. As is seen in Fig. 25, asymmetry approaches its high energy limit for the $E^{BEAM} \ge 70$ GeV. At smaller energies in the range from 10 to 40 GeV and the low p_T value, there is a significant contribution of non-asymptotic term (eq. (8)), which is most prominent at $x_A = 0.75$, and changes the shape of x_A-dependence. For energies above 70 GeV the contribution of eq. (8) is practically negligible.

Oscillation of A_N as a function of x_A is predicted for the π^0- and η-meson production in $\pi^- p^\uparrow$-collisions (see Figs. 18 and 19).

It is worth noticing that the expected maximum of $|A_N|$ for the K^+-meson production in $p^\uparrow p$-collisions is smaller than it is for the π^+-meson production. It could be related to a higher mass of constituent $\bar{s}$-quark as compared with $\bar{d}$-quark mass. The higher constituent quark mass leads to a smaller chromomagnetic momentum ($\mu \propto 1/m_q$) and a smaller asymmetry [11].

20
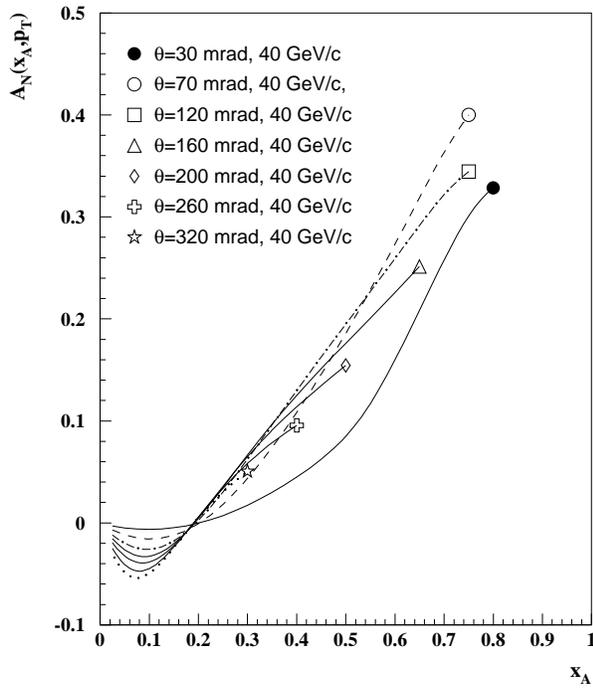
Fig. 23. Predictions of the A_N vs x_A for the π^+ production by polarized 40 GeV/c protons at the different laboratory angles.
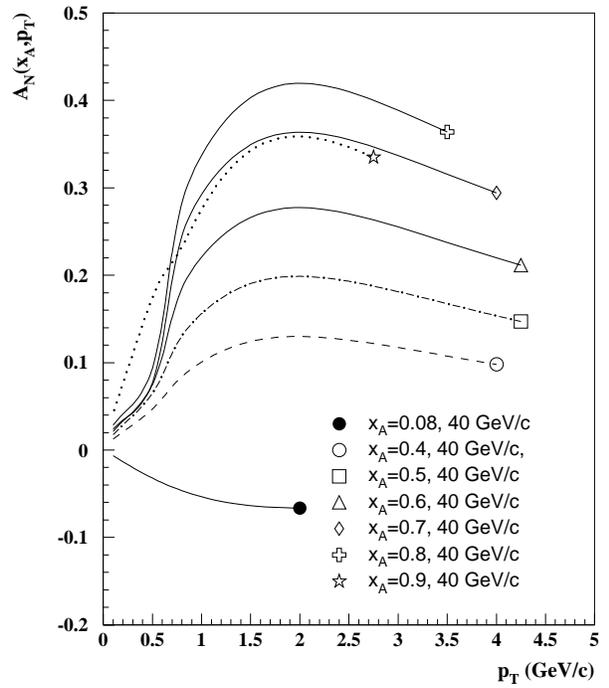
Fig. 24. Predictions of the A_N vs p_T for the π^+ production by polarized 40 GeV/c protons at the different x_A values.

Fig. 25. Predictions of the A_N vs x_A for the π^+ production by polarized protons at the different beam energies and $p_T = 0.5$ GeV/c.

21
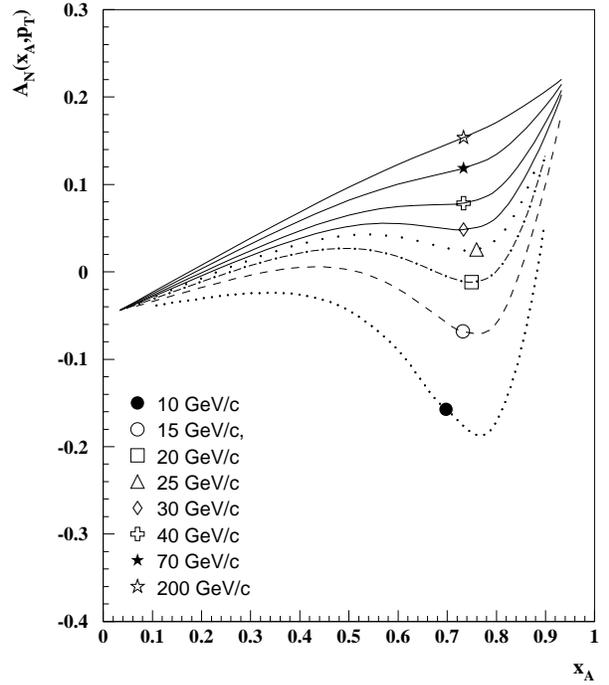
A high value of A_N is expected for the $p^\uparrow p \to K^- + X$-reaction at large x_A which contradicts some models that predict zero asymmetry [33].

Predictions for other reactions can be made using eqs. (6)-(13) and the parameters, presented in Tables 1 - 9.

It is noteworthy that for some of the reactions x_A and p_T-dependencies have already been measured with a reasonable accuracy, so it is possible to use them as polarimeters to measure beam polarization. Further improvement of experimental accuracy will make such polarimeters especially useful.

10. Conclusions

It is shown that the existing experimental data on single-spin asymmetry in inclusive reactions for meson ($\pi^\pm$, $K^\pm$, K_S^0, η) and baryon ($p, \bar{p}, \Lambda$)-production in $p^\uparrow h$-collisions can be described by a simple function of three variables ($\sqrt{s}$, p_T, x_A), where $x_A = E/E^{BEAM}$ is a new scaling variable. In the limit of high enough energy ($E^{BEAM} \geq 40$ GeV) and high p_T ($p_T \geq 1.0$ GeV/c), A_N is a function of x_A and p_T only with a precision of about 0.02-0.06, depending on a reaction type. A simple expression $A_N = F(p_T)G(x_A)$ can be used to approximate the experimental asymmetries in the above range of high energies and p_T. This scaling behavior is better fulfilled for the π^+, π^0, K^+, η, and Λ-production in $p^\uparrow p$-collisions, which takes place presumably at a quark level. Significant non-asymptotic contributions are observed for the π^- and proton production. The former has a noticeable gluon contribution, and the latter can be produced mainly from protons, existing in the initial state. Asymmetry for some hadrons has not been explored in enough detail yet to conclude about the x_A-scaling fulfillment. Additional A_N-measurements are needed at several CM angles in the central and fragmentation regions and at different energies. The bin size in x_A and p_T should be small enough to get one unbiased averaging over it, and to estimate mean values of x_A and p_T for each data point. In an ideal case, new experiments should measure x_A-dependence at fixed p_T and p_T-dependence at fixed x_A. Of interest is also a high p_T-region ($2 \leq p_T \leq 10$ GeV/c), where the decrease of asymmetry is expected with p_T rise according to some models [11,28,33].

Asymptotic dependence of A_N on x_A for most of the hadrons has a characteristic point x_0, where it intersects zero and probably changes its sign. Such behavior is in a qualitative agreement with the predictions from the models which take into account the Thomas precession and chromomagnetic forces between an outgoing quark and the rest of hadronic system. The linear dependence of A_N on x_A for most of the hadrons may indicate that the polarization of valence quark, which was kicked out from proton, is proportional to x_A or secondary hadron energy.

The use of eqs. (6) - (13) with the known parameters allows one to predict A_N in a wide range of kinematic variables and to use these predictions for the comparison with the models, to optimize future experiments and to use different reactions as polarimeters.

References

[1] Abramov V.V. et al. // Nucl. Phys. 1997, v. B492, p. 3.

[2] Bravar A. et al. // Phys. Rev. Lett. 1996, v. 77, p. 2626.

[3] Adams D.L. et al. // Phys. Rev. 1996, v. D53, p. 4747.

[4] Adams D.L. et al. // Z.Phys. 1992, v. C56, p. 181.

[5] Adams D.L. et al. // Phys. Lett. 1991, v. B264, p. 462.

[6] Saroff S. et al.// Phys. Rev. Lett. 1990, v. 64, p. 995.

[7] Apokin V.D. et al. // Phys. Lett. 1990, v. B243, p. 461.

[8] Belikov N.I. et al. - IHEP preprint 97-51, Protvino, 1997.

[9] Antille J. et al. // Phys. Lett. 1980, v. B94, p. 523.

[10] Aschman D.G. et al. // Nucl. Phys. 1978, v. B142, p. 220.

[11] Ryskin M.G. // Yad. Fiz. 1988, v. 48, p. 1114.

[12] Liang Zuo-tang and Boros C. // Phys. Rev. Lett. 1997, v. 79, p. 3608.

[13] Dragoset W.H. et al. // Phys. Rev. 1978, v. D18, p. 3939.

[14] Ayres D.S. et al. // Phys. Rev. 1977, v. D15, p. 1826.

[15] Tokarev M.V., Skoro G.P. — JINR Preprint E2-95-501, Dubna 1995.
    Musulmanbekov G.J., Tokarev M.V. — Preprint JINR E2-95-512, Dubna, 1995.

[16] Bonner B.E. et al. // Phys. Rev. 1988, v. D38, p. 729.

[17] Bravar A. et al. // Phys. Rev. Lett. 1995, v. 75, p. 3073.

[18] Bonner B.E. et al. // Phys. Rev. 1990, v. D41, p. 13.

[19] DeGrand T.A., Miettinen H. // Phys. Rev. 1981, v. D24, p. 2419.

[20] Thomas L.T. // Philos. Mag. 1927, v. 3, p. 1.

[21] Anderson B., Gustafson G. and Ingelman G. // Phys. Lett. 1979, v. B85, p. 417;
    Phys. Rep. 1983, v. 97, p. 31.

[22] Baum G. et al. // Phys. Rev. Lett. 1983, v. 51, p. 1135.

[23] Amaglobeli N.S. et al. // Yad. Fiz. 1989, v. 50, p. 695.

[24] Bonner B.E. et al. // Phys. Rev. Lett. 1988, v. 61, p. 1918.

[25] Adams D.L. et al. // Phys. Lett. 1991, v. B261, p. 201.

[26] Adams D.L. et al. - IHEP preprint 97-56, Protvino, 1997.

[27] Apokin V.D. et al. // Yad. Fiz. 1989, v. 49, p. 156.

[28] Kane G., Pumplin J., and Repko W. // Phys. Rev. Lett. 1978, v. 41, p. 1689.

[29] Arestov Yu. - in Proceedings of the 12th International Symposium on Spin Physics, Amsterdam, 1996 (World Scientific, Singapore, 1997), p. 187.

[30] Abramov V.V. // Sov. J. Nucl. Phys. 1986, v. 44, p. 856.

[31] Troshin S.M. and Tyurin N.E. // Phys. Rev. 1996, v. D54, p. 838.

[32] Fidecaro G. et al. // Phys. Lett. 1981, v. B105, p. 309.

[33] Anselmino M., Boglione M. and Murgia F. // Phys. Lett. 1995, v. B362, p. 164.

Индекс 3649